JOURNAL OF THE AMERICAN WATER RESOURCES ASSOCIATION

Vol. 55, No. 3 AMERICAN WATER RESOURCES ASSOCIATION June 2019

Does Wetland Location Matter When Managing Wetlands for Watershed-Scale Flood and Drought Resilience?

Ali A. Ameli and Irena F. Creed

Research Impact Statement: Wetlands close to the main stream network play a disproportionately important role in attenuating peakflow, while wetland location may not be important for regulating baseflow.

ABSTRACT: Wetland protection and restoration strategies that are designed to promote hydrologic resilience do not incorporate the location of wetlands relative to the main stream network. This is primarily attributed to the lack of knowledge on the effects of wetland location on wetland hydrologic function (e.g., flood and drought mitigation). Here, we combined a watershed-scale, surface–subsurface, fully distributed, physically based hydrologic model with historical, existing, and lost (drained) wetland maps in the Nose Creek watershed in the Prairie Pothole Region of North America to (1) estimate the hydrologic functions of lost wetlands and (2) estimate the hydrologic functions of wetlands located at different distances from the main stream network. Modeling results showed wetland loss altered streamflow, decreasing baseflow and increasing stream peakflow during the period of the precipitation events that led to major flooding in the watershed and downstream cities. In addition, we found that wetlands closer to the main stream network played a disproportionately important role in attenuating peakflow, while wetland location was not important for regulating baseflow. The findings of this study provide information for watershed managers that can help to prioritize wetland restoration efforts for flood or drought risk mitigation.

(KEYWORDS: watershed management; wetland; hydrologic resilience; flood; drought; Prairie Pothole Region.)

INTRODUCTION

Wetlands play an important role in maintaining hydrologic resilience of watersheds, defined as the quick return of natural hydrologic functions during and after hydrologic perturbations (Acreman and Holden 2013). Generally, riparian wetlands have been reported to reduce flood pulses by storing excess water from streams and rivers (see Bullock and Acreman 2003), and non-riparian wetlands have been found to reduce the risk of flood or drought by attenuating peakflow (Hubbard and Linder 1986; Lane and D'Amico 2010; Evenson et al. 2018) and supplying baseflow (Morley et al. 2011; Rains 2011). Despite the acknowledged role of wetlands in the hydrologic resilience of watersheds, there has been a rapid global decline in wetland area, with an average estimated global loss of wetland area since 1970 of 31% (Dixon et al. 2016). Furthermore, changes in climate, including projected warmer temperatures, altered precipitation patterns (Millett et al. 2009), and extreme precipitation events, are likely to exacerbate the negative impacts of wetland loss on watershed hydrologic resilience (Anteau et al. 2016). While wetland restoration can reverse wetland loss and promote watershed hydrologic resilience (Kusler and Kentula 1989), the effects of the number and location of restored wetlands on watershed hydrologic resilience are not well understood.

Policies to improve watershed hydrologic resilience require strategies to quantify the hydrologic functions (e.g., flood and drought mitigation) of individual wetlands — a precursor to identifying and prioritizing

Paper No. JAWRA-18-0021-P of the *Journal of the American Water Resources Association* (JAWRA). Received February 6, 2018; accepted January 31, 2019. **Discussions are open until six months from issue publication**.

School of Environment & Sustainability (Ameli, Creed), University of Saskatchewan, Saskatoon, Saskatchewan, CAN (Correspondence to Creed: irena.creed@usask.ca).

Citation: Ameli, A.A., and I.F. Creed. 2019. "Does Wetland Location Matter When Managing Wetlands for Watershed-Scale Flood and Drought Resilience?" *Journal of the American Water Resources Association* 55 (3): 529–542. https://doi.org/10.1111/1752-1688.12737.

wetlands that are especially important for protection, conservation, or restoration. However, the current inability to quantify differences in hydrologic functions of riparian vs. non-riparian wetlands or of non-riparian wetlands located at different distances from the main stream network has led to concerns over where wetland management funds and efforts should be spent (Anteau et al. 2016; Johnson and Poiani 2016).

In this study, we examined the following questions: (1) does wetland loss affect streamflow (i.e., peakflow and baseflow)? (2) is the hydrologic function of non-riparian wetlands similar to riparian wetlands? and (3) does the hydrologic function of non-riparian wetlands vary with distance from the watershed's main stream network? The cumulative effects of wetland loss on hydrologic responses at the watershed scale have been widely studied using hydrologic models (e.g., Moraghan 1993; Gleason et al. 2007; Ahmed 2013). Although these studies are useful for a general understanding of cumulative hydrologic effects of wetland loss (Johnston et al. 1990), they do not quantify the hydrologic functions of individual wetlands located in different parts of watersheds (Price et al. 2005). Quantifying the hydrologic functions of individual wetlands at different locations requires a fully distributed hydrologic model that can incorporate the geometry of each individual wetland and explicitly characterize its flux exchanges to other local and regional water bodies (Golden et al. 2014; Hayashi et al. 2016).

To answer our research questions, we combined a coupled subsurface–surface fully distributed physically based hydrologic model (Ameli and Creed 2017) with dense hydrometric measurements and historical and existing wetland inventories in the Nose Creek watershed in the Prairie Pothole Region of North America. We started by developing and testing the hydrologic model against hydrometric measurements. We then performed a series of scenario analyses to assess the impact of historically lost wetlands on stream peakflow and baseflow, and to quantify the hydrologic function (peakflow reduction, baseflow supply) of riparian wetlands and non-riparian wetlands located at different distances from the main stream network.

STUDY AREA

The Nose Creek watershed comprises 88,610 ha and is situated north of Calgary in the southern part of the province of Alberta (Canada) within the Prairie Pothole Region of North America (Figure 1). The watershed is characterized by a dry continental climate with an average precipitation of 419 mm/year and daily mean temperatures ranging from −7.1°C in January to 16.5°C in July (Government of Canada, Historical Climate Data; accessed May 2017, http://climate.weather.gc.ca/). Geology is characterized by glacial till that forms an overburden of thickness ranging from 2 to 40 m with an average of 10 m (Barker et al. 2011) and that is underlain by the Paleocene Paskapoo bedrock formation (Hayashi and Farrow 2014). Topography ranges from 1,048 to 1,336 m a.s.l., with rolling and undulating plains interspersed with wetlands (Alberta Parks 2005). Hydrography is characterized by first- to third-order streams that ultimately flow into the fourth-order stream that flows out of the watershed. Agriculture (cropland and grassland) is the dominant land use, which contributed to the 62% loss of wetland number and 79% loss of wetland area within the Nose Creek watershed.

In June 2013, the Nose Creek watershed which flows into the City of Calgary experienced a 100-year flood (1% chance of occurring in any given year). This flood was the second costliest disaster in Canadian history to date, with an estimated $6 billion dollars in damages sustained (Pomeroy et al. 2016). Smaller floods have occurred in southern Alberta in 2005 (20-year flood), 1997 (5-year flood), and 1995 (10-year flood).

Existing and Historical Wetland Inventories

Existing wetlands in the Nose Creek watershed were mapped by Ducks Unlimited Canada using manual interpretation of stereo pairs in combination with high-resolution panchromatic aerial photographs from 2006 (Ducks Unlimited Canada's Canadian Wetland Inventory; accessed February 2017, http://www.ducks.ca/initiatives/canadian-wetland-inventory/). This inventory identified 6,182 wetlands that covered 2,630 ha in the watershed (Figure 2a). It was assumed that wetland loss after 2006 was negligible relative to historical loss.

Historical (presettlement) wetlands were mapped using digital terrain analysis (Serran and Creed 2016; Serran et al. 2018). A depression probability grid was mapped using a stochastic method (Lindsay and Creed 2005) from a LiDAR digital elevation model (DEM) (1 m horizontal resolution and 15 cm vertical accuracy) acquired in October 2014. The depression probability grid was segmented into pixel groups of relatively homogeneous probability values using the multi-resolution segmentation algorithm (Baatz and Schäpe 2000). Segments with a high depression probability were classified as potential wetlands and merged to form contiguous historical wetland objects. Historical wetland objects in urban

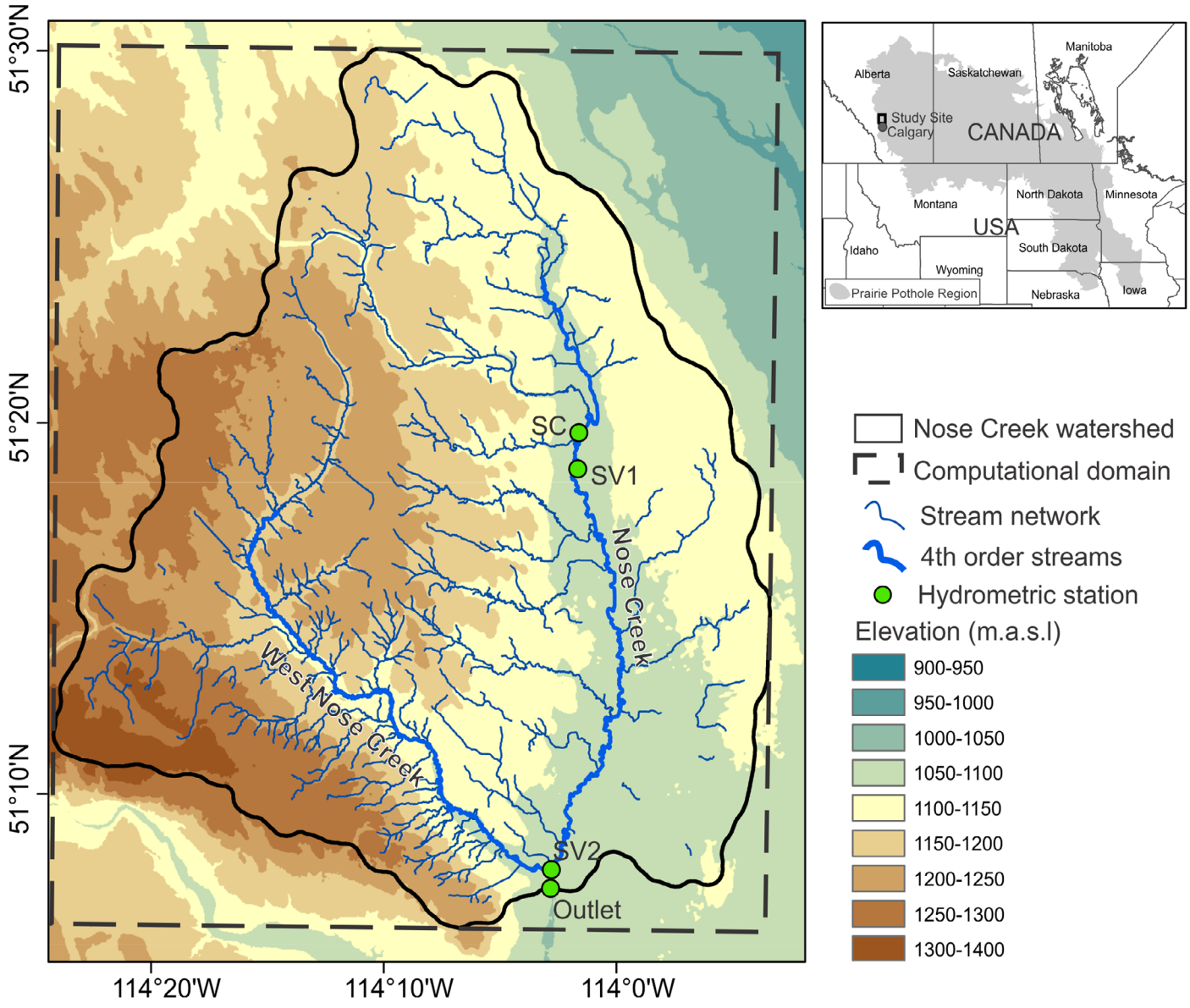

FIGURE 1. The Nose Creek watershed located north of the City of Calgary in the Province of Alberta. The rectangular boundary (dashed line) refers to the boundary of computational domain for the subsurface model. SC refers to the Nose Creek above Airdrie Water Survey of Canada hydrometric station used for model calibration; SV refers to the hydrometric stations used for model validation (SV1 is NC u/s Airdrie, SV2 is NC u/s West Nose Creek).

areas where terrain modification occurred were estimated from the classification of segmented near-infrared SPOT 6 satellite images acquired between April and July 2014; pixels with low near-infrared values (i.e., which is strongly absorbed by water) were classified as potential wetlands and merged to form contiguous historical wetland objects (Waz and Creed 2017). Urban and nonurban historical wetland objects were combined to produce a historical wetland inventory of 20,027 wetlands covering 12,500 ha (Figure 2b). Historical wetlands that were not intersected by existing wetlands were considered to be lost wetlands. Most (62% in number and 79% in area) of the lost wetlands within the watershed were temporarily lost wetlands (i.e., the topographic depressions remained on the landscape), with the potential to be restored. Details of the historical wetland mapping techniques are described in Waz and Creed (2017).

HYDROLOGIC MODEL

A three-dimensional (3D) physically based groundwater–surface water interaction model was used to

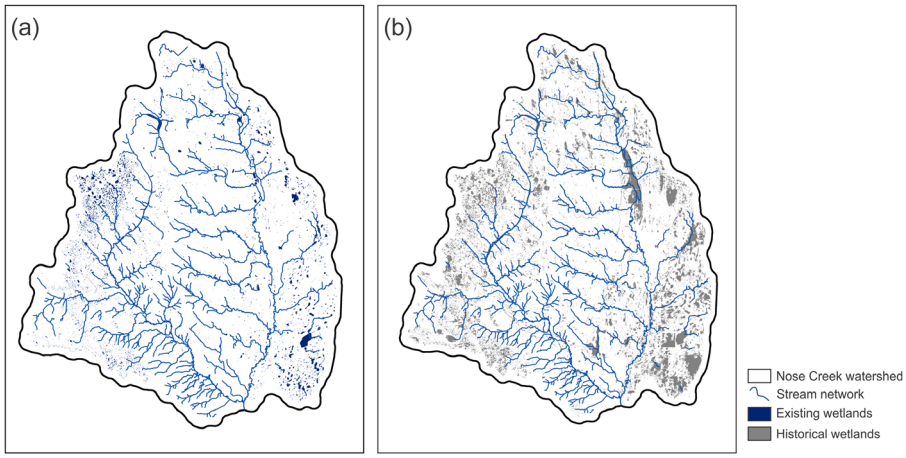

FIGURE 2. (a) Existing wetland inventory. (b) Historical wetland inventory. The blue lines refer to first- to fourth-order streams.

simulate steady-state groundwater recharge and discharge fluxes along the Nose Creek watershed. A two-dimensional (2D) physically based transient surface flow routing model was used to simulate overland flow for an eight-month period from March 1 to November 1, 2013. This period included the extreme precipitation events that led to flooding in mid-June 2013 in southern Alberta. Both models were linked to the map of existing wetlands in the Nose Creek watershed and were calibrated against measured hydrometric data.

3D Groundwater–Surface Water Interaction Model

We used the semi-analytical 3D groundwater–surface water interaction model described by Ameli and Craig (2014) to simulate steady-state local and regional groundwater flow at the Nose Creek watershed. This model has shown high efficacy and accuracy in other studies in simulating watershed-scale groundwater–surface water interaction fluxes (Ameli and Creed 2017) and groundwater age and transit time (Ameli et al. 2018). This physically based model is grid-free and satisfies the governing equation of steady-state saturated flow in each layer of an unconfined aquifer. The grid-free nature of the model allows for the explicit incorporation of the geometry of stream network as well as riparian and non-riparian wetlands of different sizes, and thus facilitates the assessment of the hydrologic influences of each individual wetland on the subsurface hydrology (e.g., groundwater fluxes) of the watershed.

A rectangular boundary around the Nose Creek watershed was used as the subsurface computational domain (Figure 1). No-flow boundary conditions were imposed along the four sides of the rectangular computational domain. The computational domain in the vertical direction consisted of a two-layer system represented by permeable glacial sediments with a thickness of 10 m overlaying a potentially less permeable bedrock formation; this treatment is consistent with the Nose Creek watershed geology. The top boundary of the computational domain was the DEM-based ground surface. The no-flow bottom boundary of the computational domain was assumed to be at $Z = 0$. This treatment led to a varying aquifer thickness from 1,048 to 1,336 m.

The model assumed a hydraulic connection between water level in the wetland and the surrounding groundwater table. This assumption is supported by conceptual understanding and measurements of groundwater–wetland interactions within the Canadian portion of Prairie Pothole Region (van der Kamp and Hayashi 2009). For example, at the St. Denis National Wildlife Area 500 km east of the Nose Creek watershed, the long-term maximum difference between the wetland water level and the groundwater level, at a piezometer located 7 m from the wetland edge, was <10 cm. The flow in the unsaturated zone (above the groundwater table) was assumed to be vertical. This assumption will likely have little impact on our results given the small depth to groundwater table (unsaturated zone thickness) observed in the Nose Creek watershed (see Barker et al. 2011). In addition, given the small rainfall to evapotranspiration ratio in the Nose Creek watershed, typical of a dry continental climate, there is a small likelihood of the occurrence of lateral water movement in the shallow unsaturated zone through subsurface stormflow, which is typically observed in humid forested landscapes with permeable soils and a relatively large rainfall to evapotranspiration ratio (c.f. Ameli et al. 2015). In the groundwater–surface water interaction model, the water level at each intact wetland was considered to be equal to the

median of the long-term water level in the wetland simulated using the surface flow routing model during the eight-month study period; this water level was then used as the constant head boundary condition at the intact wetland. Temporarily lost wetlands were treated as non-wetland areas or regular land surface where no constant head boundary condition was imposed.

The model used a free-surface boundary condition to determine the location of the groundwater table and groundwater discharge zones. The free-surface boundary condition ensures a robust determination of the groundwater table configuration with the ability to sufficiently quantify local and regional groundwater flow patterns. The free surface condition was iteratively imposed using the recharge–water table depth relation algorithm presented in Ameli and Craig (2014) that creates a spatially variable recharge rate and enables delineation of discharge areas. In this algorithm, the location of the groundwater table is guessed in the first iteration. The iterations continue and the location of groundwater table is modified until the pressure head along the a priori unknown groundwater table location converges to zero. At each iteration, the recharge condition was applied along the groundwater table at non-wetland recharge areas, and as stated above, the constant head boundary condition was applied along the intact wetlands. Recharge rate was constant in most parts of the non-wetland recharge areas (with a rate equal to the maximum recharge rate) but smoothly decreased where the groundwater table depth approached zero (e.g., close to discharge areas). Once the groundwater table converged, the continuous function for groundwater (recharge and discharge) fluxes at wetland and non-wetland areas was determined. The mathematical formulation, solution parameters, implementation of boundary conditions of the semi-analytical model, and the equations for calculating groundwater recharge–discharge fluxes are further explained in the Supporting Information (Text S1).

Here, the semi-analytical model was calibrated using: (1) saturated hydraulic conductivity of the top layer (glacial sediment) of the unconfined aquifer; (2) saturated hydraulic conductivity of the bottom layer (bedrock) of the unconfined aquifer; and (3) maximum recharge rate. The model performance was assessed for its ability to map groundwater discharge–recharge areas and fluxes within the Nose Creek watershed. We compared the simulated groundwater discharge–recharge areas and fluxes to one derived from hydrometric measurements. We used measurements of hydraulic heads in 474 artesian groundwater wells installed in the bedrock and screened 30–80 m below the land surface (http://aep.alberta.ca/water/reports-data/alberta-water-well-information-database/) and used a kriging approach to map the potentiometric surface throughout the entire watershed. Groundwater discharge and recharge areas were inferred as areas where potentiometric surface is above and below land surface, respectively. The distance of potentiometric surface from the land surface refers to the relative value of recharge and discharge fluxes, with larger negative distances (above land surface) representing larger discharge fluxes and larger positive distances (below land surface) representing larger recharge rates (Barker et al. 2011). The three parameters of the groundwater–surface water interaction model were adjusted to acquire the largest correlation coefficient between simulated groundwater discharge–recharge fluxes and the inferred groundwater discharge–recharge fluxes from the measured potentiometric surface.

2D Transient Surface Flow Routing Model

The 2D transient overland flow simulation was performed using the fill-and-spill surface flow routing simulator within the numerical physically based HydroGeoSphere model (Therrien et al. 2008). A no-flow boundary condition was assigned to the watershed's boundary (Figure 1). The 2D surface of the watershed was discretized into 104,439 grid points (207,248 triangular elements). Such high-resolution discretization of the computational domain ensures the incorporation of the geometry of the stream network and riparian and non-riparian wetlands of different sizes (as small as 0.01 ha) in the computational domain. The surface flow routing model uses a depth-integrated diffusion-wave approximation of the Saint Venant equation which allows for an explicit physically based simulation of wetland flow dynamics and wetland feedbacks with the stream network. Once a hydrologic feature (stream or wetland) fills, the Diffusion-Wave equation governs the lateral movement of the water along the land surface between hydrologic features. The governing equation and mathematical formulation of surface flow routing dynamics are further explained in the Supporting Information (Text S2).

The inputs to the surface flow routing model included measured daily air temperature, rainfall, snowfall, and estimated evapotranspiration from data collected between January 1 and November 1, 2013 at the Neir Alberta Environment Drought Monitoring station (located 10 km north of the Nose Creek watershed) (http://agriculture.alberta.ca/acis/alberta-weather-data-viewer.jsp). The input to the model also included the steady-state spatially distributed groundwater recharge and discharge fluxes obtained using the 3D groundwater–surface water interaction

model. The first two months of the model simulation represented the warm-up period and the remaining eight months (March 1–November 1, 2013) represented the study period.

The 2D surface flow model was calibrated using: (1) two Manning roughness coefficients (Manning et al. 1890) for cropland and grassland surfaces; (2) two rill depths for non-wetland surfaces and wetland surfaces; and (3) one snowmelt-related parameter including snow density. Rill depth represents the amount of storage that must be filled before any lateral surface flow can occur (Therrien et al. 2008). Rill depth is large for wetland surfaces as a large amount of water is needed to fill the wetland before it spills and lateral surface flow occurs. Rill depth is smaller for regular land surfaces and temporarily lost wetlands, where a smaller amount of storage can lead to lateral surface flow. Rill depth for a given intact wetland corresponded to the depth of the wetland pour point relative to the lowest depth of the wetland. The median depth of the wetland pour point relative to the lowest depth of the wetland was estimated (using ArcGIS version 10.5; ESRI, Redlands, California, USA) as 4.6 m for all existing wetlands along the Nose Creek watershed. The five parameters of the surface flow routing model were adjusted to acquire the best corroboration between simulated and observed daily streamflow values during the study period at Nose Creek above the Airdrie Water Survey of Canada hydrometric station (Government of Canada, Hydrometric Station and Network Data; accessed June 2017, https://wateroffice.ec.gc.ca/mainmenu/station_and_network_data_index_e.html) (SC in Figure 1).

Coupled Subsurface–Surface Model

The 3D groundwater–surface water interaction model and 2D surface flow routing model were coupled in two ways to incorporate feedbacks between groundwater and surface water systems. First, the steady-state spatially distributed groundwater recharge rate and groundwater discharge fluxes obtained using the groundwater–surface water interaction model were used as inputs to the surface flow routing model. Second, the median long-term water level in each intact wetland, simulated using the surface flow routing model during the study period, was used as a constant head boundary condition at the intact wetland in the groundwater–surface water interaction model. Five iterations between the two models were required to ensure a full coupling; coupling code was generated in MATLAB 9.1 (MathWorks, Inc., Natick, Massachusetts, USA). The performance of the coupled model in the validation phase was evaluated by comparing simulated streamflow against streamflow measurements at two hydrometric stations in the Nose Creek watershed including SV1 (Nose Creek u/s Airdrie) and SV2 (Nose Creek u/s West Nose Creek) (the location of stations are shown in Figure 1).

Wetland Scenarios

The calibrated coupled subsurface–surface hydrologic model was used to perform a series of wetland scenario analyses to assess the impact of wetland loss on stream peakflow and baseflow, and to quantify the hydrologic functions (peakflow reduction, baseflow supply) of wetlands located at different distances relative to the main stream network. For different wetland scenarios, hydrologic responses were characterized using: (1) daily streamflow values at the watershed outlet; (2) peakflow or the largest streamflow event over the eight-month study period at the watershed outlet; (3) cumulative streamflow at the watershed outlet at the end of the study period; and (4) total baseflow to the entire length of the main stream network (fourth-order streams; see blue lines in Figure 3b).

In the first set of wetland scenarios, we applied the hydrologic model to the historical wetland inventory (Figure 2b) and compared the hydrologic responses between this historical wetland model and the existing wetland model (the calibrated model) to characterize changes in hydrologic responses as a result of historical wetland loss. In the second set of wetland scenarios, we examined the importance of non-riparian wetlands on attenuating peakflow and supplying baseflow by randomly removing a different percent of non-riparian wetlands from the historical wetland model including 25% ($loss_{25}$), 50% ($loss_{50}$), 75% ($loss_{75}$), and 100% ($loss_{100}$) loss of non-riparian wetlands (Figure 3a). Riparian wetlands were identified as wetlands with a majority of their area lying within a riparian area defined according to environmental reserve setback zones (determined by City of Calgary), which are 6, 30, 50, and 50 m around first-, second-, third-, and fourth-order streams, respectively (Graf et al. 2016).

In the third set of wetland scenarios, we removed wetlands located greater than 0 m ($dist_0$), 100 m ($dist_{100}$), 2,000 m ($dist_{2000}$), and 4,000 m ($dist_{4000}$) from the main stream network (fourth-order streams) (Figure 3b). This systematic removal of wetlands enabled us to explore how the hydrologic functions (peakflow reduction, baseflow supply) of wetlands varied with distance from the main stream network. For example, the difference between the hydrologic responses of the $dist_{2000}$ and $dist_{4000}$ scenarios reveal the hydrologic functions of wetlands located between 2,000 m and 4,000 m from the main stream network.

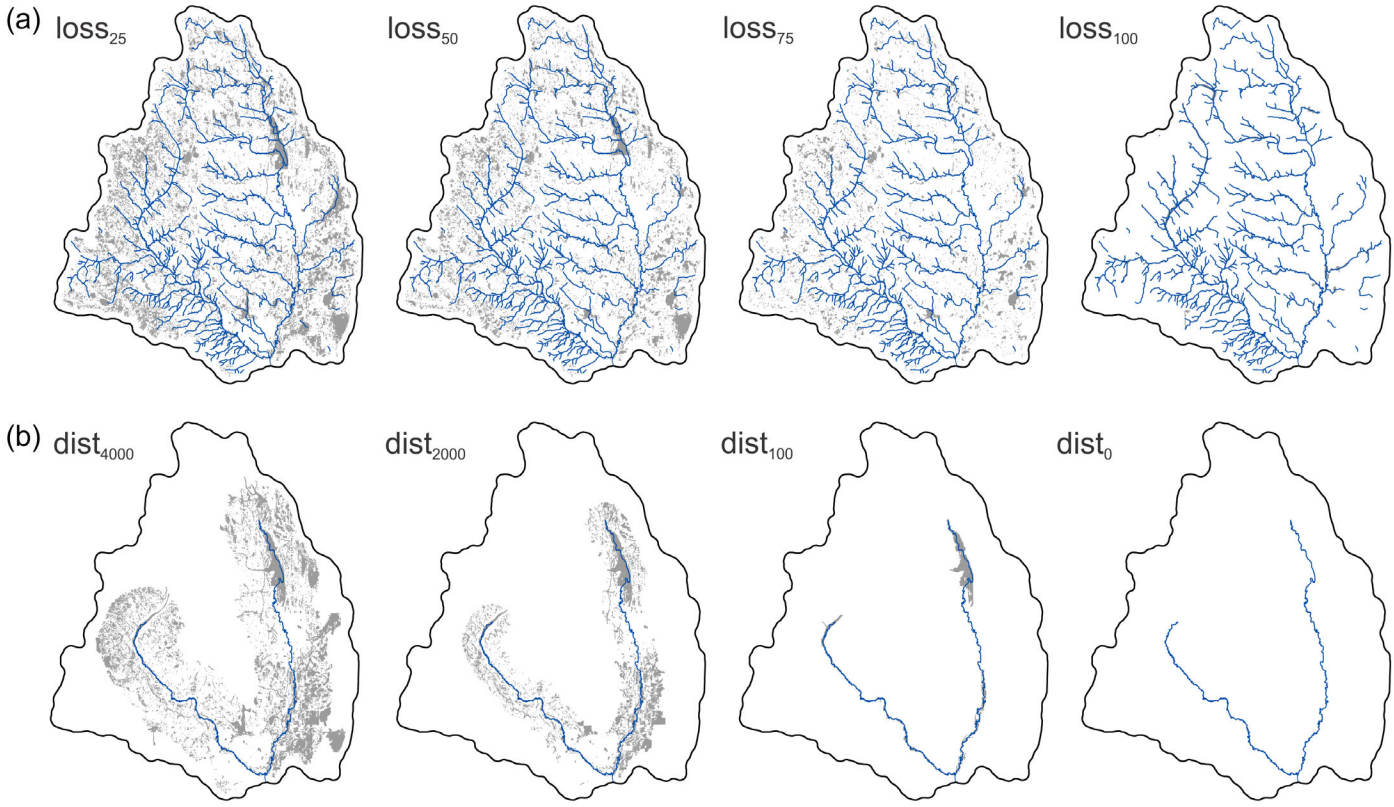

FIGURE 3. Maps of wetlands used in the scenario analysis experiments. (a) Scenarios A: non-riparian wetlands were randomly removed at the rate of 25% ($loss_{25}$), 50% ($loss_{50}$), 75% ($loss_{75}$), and 100% ($loss_{100}$). Here, the blue line refers to entire stream network. (b) Scenarios B: wetlands located greater than specified distances of major stream network were removed. Wetlands located greater than 4,000, 2,000, 100, and 0 m of main stream network were removed in scenarios $dist_{4000}$, $dist_{2000}$, $dist_{100}$, and $dist_0$, respectively. Here, the blue line refers to the main stream network (i.e., the fourth-order stream). In all scenarios, wetlands were removed from the historical wetland inventory.

RESULTS

Calibration of Groundwater–Surface Water Interaction Model

Through manual calibration, the saturated hydraulic conductivities of the top layer (glacial sediment) and bottom layer (bedrock) of the unconfined aquifer were calculated as 0.075 and 0.05 m/day, respectively, and the maximum recharge rate was calculated as 18.5 mm/year. The values of the physical parameters calibrated by the model were consistent with the estimated values in other studies in the Nose Creek watershed. For example, Barker et al. (2011), using a water-balance method, suggested that the groundwater recharge rate within the Nose Creek watershed varies spatially between 5 and 50 mm/year. Niazi et al. (2017), using groundwater chloride concentrations, estimated that the groundwater recharge rate varies spatially from 7.5 mm/year to 37 mm/year and the bedrock saturated hydraulic conductivity varies spatially between 0.003 and 0.085 m/day within the west portion of the Nose Creek watershed.

The simulated map of groundwater discharge–recharge fluxes along the entire watershed was consistent with the map of groundwater discharge–recharge fluxes inferred from the measured potentiometric surface in piezometric wells, with a correlation coefficient of 0.61 (Figure 4). The modeled and inferred groundwater discharge fluxes along the main stream network were also consistent with a correlation coefficient of 0.95. The area of the watershed that was simulated as a discharge zone was 15.02% and the area of watershed inferred as discharge zone from measured potentiometric surface was 15.11%.

Calibration of Surface Flow Routing Model

Through manual calibration, (1) Manning roughness coefficients were calibrated as 0.15 $s/m^{1/3}$ for cropland and 0.05 $s/m^{1/3}$ for grassland, (2) rill depths were calibrated at 0.001 m for non-wetland surfaces and 4.9 m for wetland surfaces, and (3) snow density

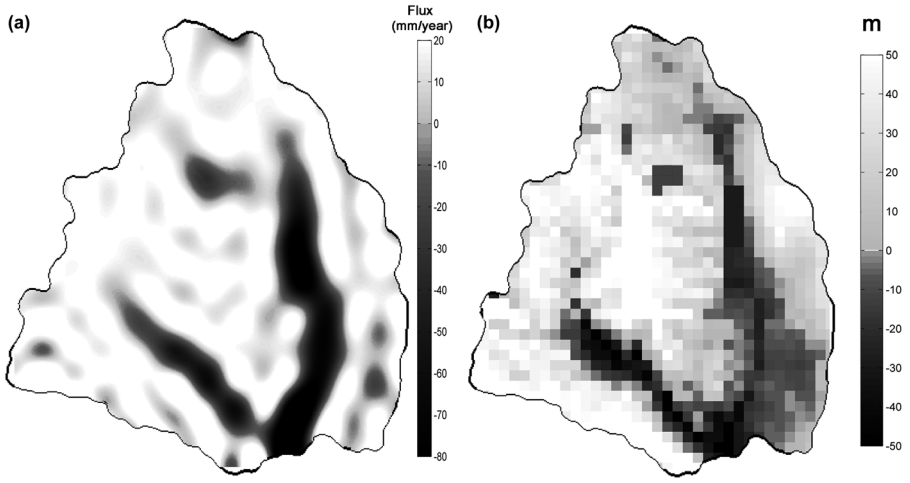

FIGURE 4. Comparison between simulated and observed groundwater discharge/recharge fluxes. (a) Simulated groundwater discharge (dark surfaces) and recharge (light surfaces) fluxes (mm/year) based on the existing wetland inventory. (b) Observed distance of potentiometric surface from land surface (m) based on measurements of hydraulic heads in 474 artesian groundwater wells installed in the bedrock that were kriged to estimate the potentiometric surface, with larger negative distances inferred as larger discharge fluxes (dark surfaces) and larger positive distances inferred as larger recharge rates (light surfaces). The correlation coefficient between modeled and inferred groundwater fluxes is 0.61 along the entire watershed and is 0.95 along the main stream network.

was calibrated at 400 kg/m^3. The calibrated Manning roughness coefficients were consistent with the suggested values for crop land and grassland covers (see Phillips and Tadayon 2006). The calibrated rill depth for wetland surfaces was consistent with the median of the depths of the wetland pour point relative to the lowest point in the wetland which was estimated at 4.6 m in an independent analysis using ArcGIS. The calibrated value for snow density (400 kg/m^3) was consistent with observed values at other watersheds with similar climates as the Nose Creek watershed within the Canadian portion of the Prairie Pothole Region (see Coles 2017).

The ability of the calibrated surface flow routing model to simulate observed daily streamflow at the Nose Creek above Airdrie station during the study period between March 1 and November 1, 2013 was appropriate, with R^2 and Nash–Sutcliffe (NS) values of 0.84 and 0.82, respectively (Figure 5a). The calibrated model was able to capture the largest streamflow that occurred on June 20, 2013 (the day of the Calgary flood), but the simulated cumulative streamflow at the end of study period within Nose Creek above Airdrie station (SC) was 10% smaller than the observed cumulative streamflow.

Validation of the Coupled Subsurface–Surface Flow Model

In the validation phase, the simulated daily streamflow during the study period was comparable to observed streamflow at the SV1 (R^2 = 0.87 and NS = 0.86) and SV2 (R^2 = 0.91 and NS = 0.85) hydrometric stations (Figure 5b,5c). With the coupled surface–subsurface flow model able to capture the observed streamflow and groundwater fluxes, we assessed the effect of different scenarios of wetland loss on stream peakflow and baseflow toward the main stream network. In these wetland loss scenario analyses, the eight calibrated parameters remained constant.

Hydrologic Functions of Historically Lost Wetlands

The comparison of watershed-scale groundwater discharge fluxes between the historical wetland model and existing wetland model suggests that wetland loss resulted in a decrease of groundwater discharge area from 15.6% to 15.02% (Figure 6). In addition, the pattern of groundwater discharge flux rate along the watershed slightly changed. The total groundwater baseflow discharged into the main stream network (fourth-order streams) decreased by 6%. Comparison of the simulated hydrograph at the watershed outlet between the historical wetland model and existing wetland model showed that stream peakflow, which occurred on June 20, 2013 in both models, increased by 19% and cumulative streamflow at the end of study period increased by 17% with wetland loss (Figure 6).

Hydrologic Functions of Non-Riparian Wetlands

Stream peakflow and cumulative streamflow at the watershed outlet increased with decreases in the area of

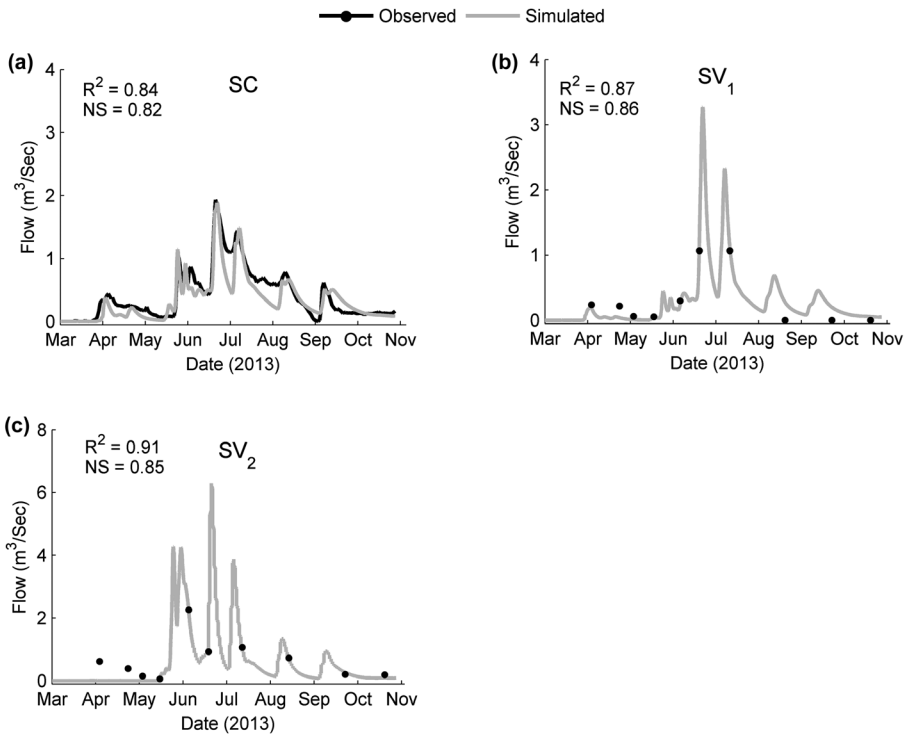

FIGURE 5. Performance of the hydrologic model with existing wetland inventory against daily streamflow measurements from March 1 to November 1, 2013. (a) Model performance during calibration phase at SC hydrometric station. Model performance during validation phase at (b) SV1 station and (c) SV2 station (see Figure 1 for station locations). The largest streamflow in all stations occurred on June 20, 2013 (on the same day as the Calgary flood).

non-riparian wetlands (Figure 7a,7b — left panels). Large increases were observed between the 50% and 75% removal scenarios of non-riparian wetlands. As the area of non-riparian wetland removal increased from 5,960 ha ($loss_{50}$) to 8,720 ha ($loss_{75}$), the relative increase in stream peakflow increased from 1.5% to 13% and in cumulative streamflow increased from 4.5% to 15%. These values were calculated relative to stream peakflow and cumulative flow in the historical wetland model.

Total baseflow discharged to the entire length of the main stream network decreased systematically with increasing area of non-riparian wetlands removed (Figure 7c). Removal of 3,120 ha ($loss_{25}$), 5,960 ha ($loss_{50}$), 8,720 ha ($loss_{75}$), and 11,280 ha ($loss_{100}$) of non-riparian wetlands led to relative decreases of 3.2%, 4.6%, 5.7%, and 8.9% in total baseflow discharged to the main stream network, respectively. These values were calculated relative to total baseflow to the main stream network in the historical wetland model.

Hydrologic Functions of Distal and Proximal Wetlands

Figure 7 (right panels) shows the impact of the removal of wetlands located greater than specified distances (0, 100, 2,000, and 4,000 m) from the main stream network on stream peakflow and stream baseflow. Removal of 8,959 ha of wetlands located >2,000 m ($dist_{2000}$) from the main stream network led to relative increases of 4% in stream peakflow and 6% in cumulative streamflow. Also, the removal of 11,391 ha of wetlands located >100 m ($dist_{100}$) from the fourth-order streams led to relative increases of 5% in the stream peakflow and 6.8% in cumulative streamflow. These values were calculated relative to stream peakflow and cumulative flow in the historical wetland model.

This systematic removal of wetlands enabled us to explore how much stream peakflow and baseflow vary with the removal of wetlands located in different parts of the watershed. Removal of wetlands within 100 m of the main stream network had a large impact on stream peakflow and cumulative flow at the watershed outlet (Table 1). While the removal of wetlands located farther than 4,000 m from the main stream network increased stream peakflow at a rate of 1.61 m^3/day per unit wetland area (ha), removal of wetlands located within 100 m of the main stream network increased stream peakflow at a rate of 268 m^3/day/ha. Similarly, removal of wetlands located farther than 4,000 m from the main stream network

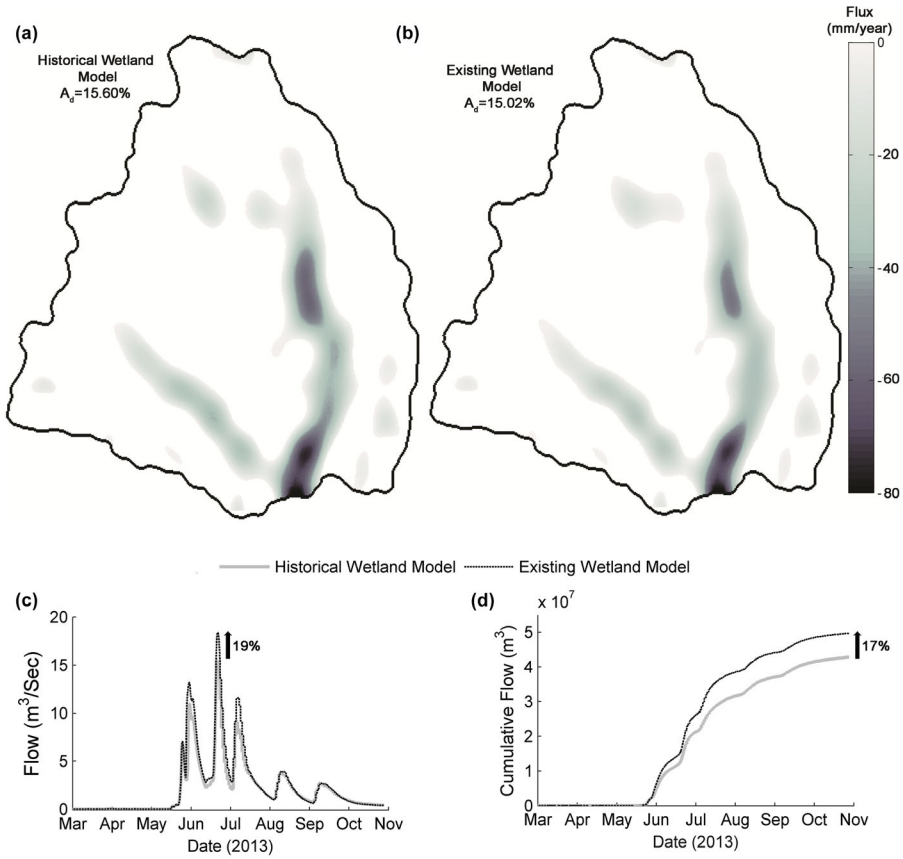

FIGURE 6. Groundwater steady-state discharge flux pattern (mm/year) for (a) historical wetland model and (b) existing wetland model. A_d is discharge area expressed as a percentage of watershed area. The total groundwater baseflow discharged into the main stream network (fourth-order streams) decreased by 6% with the loss of wetlands between historical and existing wetland cases. Watershed outlet (c) simulated daily streamflow hydrograph for historical and existing wetland models during the study period between March 1 and November 1, 2013, and (d) simulated cumulative daily streamflow for historical and existing wetland models.

increased cumulative streamflow at the watershed outlet at a rate of 187 m^3/ha, but removal of wetlands located within 100 m of the main stream network increased cumulative streamflow at a rate of 6,863 m^3/ha. Removal of wetlands located at different distances from the main stream network reduced total baseflow discharged into the entire length of the main stream network at an almost constant rate (from 0.0015 to 0.0017 m^3/day/ha; Table 1).

DISCUSSION

Wetlands contribute to the hydrologic resilience of watersheds by reducing stream peakflow and supplying baseflow (Rains et al. 2015; Cohen et al. 2016). Nonetheless, most hydrologic models cannot quantify the hydrologic functions of individual (lost and existing) wetlands, which is required for identifying wetlands that are important to protect or restore to enhance the hydrologic resilience of watersheds. The coupled subsurface–surface flow model presented in this paper incorporates the geometry of individual wetlands, regardless of their size, and assesses the influence of each wetland on watershed-scale subsurface–surface hydrologic responses. This physically based model captured the observed stream baseflow and peakflow in the wetland-dominated Nose Creek watershed in response to extreme precipitation events that led to the catastrophic 100-year flood within the watershed and downstream cities. We then used this subsurface–surface hydrologic model to explore long-standing questions related to the identification of areas of the watershed where wetland restoration and protection should be prioritized to improve watershed hydrologic resilience.

Hydrologic Function of Historically Lost Wetlands During an Extreme Flooding

Within the Nose Creek watershed, wetland loss led to an increase in the volume of water discharged toward

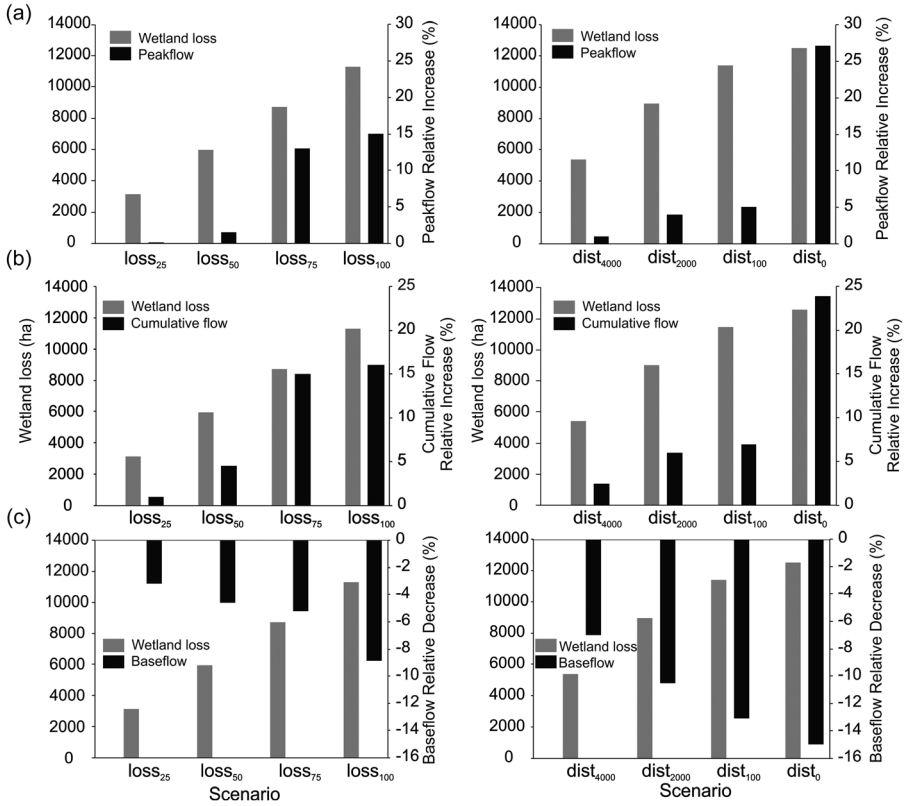

FIGURE 7. Relative changes in hydrologic responses for different wetland loss scenarios compared to the historical wetland model in (a) stream peakflow at the watershed outlet, which occurred during the Calgary flood on June 20, 2013, (b) watershed outlet cumulative streamflow at the end of the study period, and (c) total baseflow discharged into the entire length of the main stream network (fourth-order streams).

TABLE 1. Hydrologic functions of wetlands located at different distances of the main stream network (fourth-order streams): $dist_{4000}$ evaluates the hydrologic functions of wetlands located farther than 4,000 m from the main stream network; $dist_{4000}$–$dist_{2000}$ evaluates the hydrologic functions of wetlands located between 4,000 and 2,000 m from the main stream network; $dist_{2000}$–$dist_{100}$ evaluates the hydrologic functions of wetlands located between 2,000 and 100 m from the main stream network; and $dist_{100}$–$dist_0$ evaluates the hydrologic functions of wetlands located within 100 m of the main stream network.

Wetland loss scenario	Wetland distance (L) from main stream network (m)	Peakflow increase (m^3/day) per wetland area (ha)	Cumulative flow increase (m^3) per wetland area (ha)	Baseflow decrease (m^3/day) per wetland area (ha)
$dist_{4000}$	$L > 4{,}000$	1.61	187	0.0017
$dist_{4000}$–$dist_{2000}$	$4{,}000 > L > 2{,}000$	3.89	444	0.0015
$dist_{2000}$–$dist_{100}$	$2{,}000 > L > 100$	4.32	459	0.0015
$dist_{100}$–$dist_0$	$0 < L < 100$	268	6,863	0.0017

the City of Calgary during the flood that occurred in June 2013. Our modeling results showed that the volume of water discharged at the outlet of the Nose Creek watershed during the week of flood (June 17–24, 2013) could have been 0.8 million m^3 smaller if all historically lost wetlands were present. While this volume of water was equivalent to 15% of the total volume of water (5.31 million m^3) that was discharged from the Nose Creek watershed toward the City of Calgary during the week of flood, this volume was equivalent to only 0.2% of the total volume of water (540 million m^3) discharged toward the City of Calgary from all sources during the week of the flood. The latter was calculated as the measured cumulative streamflow during the week of flood within the Bow River at the Calgary hydrometric station located in downtown Calgary.

Our modeling results also showed that the historical loss of wetlands decreased baseflow toward the main stream network by 6%. This corroborates the findings of Ameli and Creed (2018) that showed that the loss of wetlands over time decreases baseflow toward local surface water bodies in a large 400,000 ha wetland-dominated watershed. Reductions in the ability of wetlands to attenuate peakflow and supply baseflow negatively affect the hydrologic resilience of a watershed, increasing the risk of floods and droughts.

Where Should Wetlands Be Restored to Enhance Watershed Hydrologic Resilience?

Loss of hydrologic resilience can be mitigated through wetland restoration (Cohen et al. 2016), but the effectiveness of restoration depends, at least partly, on where wetlands are restored relative to main stream network (USEPA 2015). Our modeling results showed that all wetlands contribute to a reduction in peakflow and cumulative flow, but wetlands located in different locations relative to main stream network attenuate stream peakflow and cumulative flow at significantly different rates. There was a greater increase in stream peakflow and cumulative flow with the loss of wetlands located within 100 m of the main stream network than when wetlands located farther than 100 m of the main stream network were lost (Table 1). For example, peakflow reduction of each hectare of wetland located within 100 m of the main stream network (268 m^3/day) was more than 165 times larger than this measure for each hectare of wetlands located farther than 4,000 m of the main stream network (1.61 m^3/day). These findings imply that riparian wetlands and wetlands located at close proximity (<100 m) to main stream network should be prioritized for restoration or protection in watersheds where controlling flooding is important. Nonetheless, non-riparian wetlands still have the potential to contribute to stream peakflow and cumulative flow reduction. A threshold (approximately 50%) of non-riparian wetland loss number existed, above which further loss of non-riparian wetlands disproportionately increased stream peakflow and cumulative flow.

On the other hand, our modeling results showed that wetlands located in different parts of a watershed contribute almost equally to baseflow supply to the main stream network. Baseflow supply to local water bodies can help to mitigate drought by improving low-flow during extremely dry and/or warm periods (Min et al. 2010; Golden et al. 2015).

Implication for Wetland Management and Policy

Wetland restoration is often subject to many restrictions regarding where wetlands can be restored (e.g., ownership of the wetlands, owner's willingness to restore the wetland, etc.) (Clare and Creed 2014). Identifying wetlands that could disproportionately enhance a watershed hydrologic resilience provides watershed managers with important science-based tools to identify priority wetlands, and to negotiate with the land owners of these priority wetlands, to restore them. Our modeling results suggest that if the management focus is on flood mitigation, wetlands located at close proximity to main stream network would be optimal options to be restored, but if the focus is on drought mitigation, any wetland would be optimal to restore.

In addition, watershed managers can incorporate the location of the wetland relative to the stream network into watershed management plans to help meet watershed management objectives (e.g., Creed et al. 2017; Accatino et al. 2018). For example, the Government of Alberta switched from a no-net loss area-based policy to a no-net loss functional-based policy (Government of Alberta 2013). This policy requires the development of science-based tool to assign scores to each wetland based on its ability to provide ecological health, hydrologic function, and water purification functions (Creed et al. 2017). Direct quantification of the hydrologic function (stream peakflow reduction and baseflow supply) of individual wetlands could inform the assignment of science-based scores on hydrologic function to wetlands based on where wetlands are located within the watershed. High-resolution physically based models (like the one used in this paper) are now available to quantify the hydrologic influences of individual wetlands on watershed hydrologic resilience, to inform the assignment of science-based scores to these wetlands. Such information is required to design watershed management plans and be better positioned to achieve watershed hydrologic resilience that will reduce risk of floods and droughts.

CONCLUSION

Effective wetland restoration strategies require knowledge to identify which wetlands should be prioritized for restoration. The physically based coupled subsurface–surface flow model presented in this paper enables wetland managers to develop a predictive understanding of how the location of wetlands within a watershed affects their ability to improve

watershed hydrologic resilience. In the study watershed, the modeling results show that wetlands located in the vicinity of main stream networks disproportionately reduce peakflow and, subsequently, the risk of flooding during extreme precipitation events. But the peakflow attenuation function of wetlands decreases as the distance from the main stream network increases. Wetland restoration scenarios in which higher proportions of wetlands close to main stream networks are restored are more likely to promote watershed hydrologic resilience against flooding compared to alternative scenarios in which lower proportions of proximal wetlands are restored, regardless of the total area of restored wetlands. Such high-resolution physically based models can be used to predict the hydrologic function of individual wetlands located at different parts of watersheds under different flood projections (e.g., 20-, 50-, 100-year floods), and to inform watershed management plans.

SUPPORTING INFORMATION

Additional supporting information may be found online under the Supporting Information tab for this article: A description of the mathematical formulation of the model.

DATA AVAILABILITY

Data are available upon request from the corresponding author.

ACKNOWLEDGMENTS

We acknowledge funding of the Natural Sciences and Engineering Research Council of Canada (NSERC) Discovery Grant (Grant #06579-2014 RGPIN) and Alberta Environment and Parks Watershed Resiliency and Restoration Program Grant to IFC. We appreciate the constructive comments by three anonymous reviewers and the associate editor of the Journal of American Water Resources Association.

LITERATURE CITED

Accatino, F., I.F. Creed, and M. Weber. 2018. "Landscape Consequences of Aggregation Rules for Functional Equivalence in Compensatory Mitigation Programs." *Conservation Biology* 32 (3): 694–705.

Acreman, M., and J. Holden. 2013. "How Wetlands Affect Floods." *Wetlands* 33 (5): 773–86.

Ahmed, F. 2013. "Cumulative Hydrologic Impact of Wetland Loss: Numerical Modeling Study of the Rideau River Watershed, Canada." *Journal of Hydrologic Engineering* 19 (3): 593–606.

Alberta Parks, 2005. "*Natural Regions and Sub-Regions of Alberta*." Alberta Parks, Government of Alberta, Edmonton, Alberta, Canada.

Ameli, A.A., J. Craig, and J. McDonnell. 2015. "Are All Runoff Processes the Same? Numerical Experiments Comparing a Darcy-Richards Solver to an Overland Flow-Based Approach for Subsurface Storm Runoff Simulation." *Water Resources Research* 51 (12): 10008–28.

Ameli, A.A., and J.R. Craig. 2014. "Semianalytical Series Solutions for Three-Dimensional Groundwater-Surface Water Interaction." *Water Resources Research* 50 (5): 3893–906.

Ameli, A.A., and I.F. Creed. 2017. "Quantifying Hydrologic Connectivity of Wetlands to Surface Water Systems." *Hydrology & Earth System Sciences* 21 (3): 1791–808.

Ameli, A.A., and I.F. Creed. 2018. "Groundwaters at Risk: Wetland Loss Changes Sources, Lengthens Pathways, and Decelerates Rejuvenation of Groundwater Resources." *Journal of the American Water Resources Association*. https://doi.org/10.1111/1752-1688.12690.

Ameli, A.A., C.P. Gabrielli, U. Morgenstern, and J. McDonnell. 2018. "Groundwater Subsidy from Headwaters to Their Parent Water Watershed: A Combined Field-Modeling Approach." *Water Resources Research* 54: 5110–25. https://doi.org/10.1029/2017WR022356.

Anteau, M.J., M.T. Wiltermuth, M.P. van der Burg, and A.T. Pearse. 2016. "Prerequisites for Understanding Climate-Change Impacts on Northern Prairie Wetlands." *Wetlands* 36 (2): 299–307.

Baatz, M., and A. Schäpe. 2000. "Multiresolution Segmentation: An Optimization Approach for High Quality Multi-Scale Image Segmentation." *Angewandte Geographische Informationsverarbeitung* XII: 12–23.

Barker, A., J. Riddell, S. Slattery, L. Andriashek, H. Moktan, S. Wallace, S. Lyster, G. Jean, G. Huff, and S. Stewart. 2011. "Edmonton–Calgary Corridor Groundwater Atlas." *Energy Resources Conservation Board, ERCB/AGS Information Series* 140: 90.

Bullock, A., and M. Acreman. 2003. "The Role of Wetlands in the Hydrological Cycle." *Hydrology and Earth System Sciences Discussions* 7 (3): 358–89.

Clare, S., and I.F. Creed. 2014. "Tracking Wetland Loss to Improve Evidence-Based Wetland Policy Learning and Decision Making." *Wetlands Ecology and Management* 22 (3): 235–45.

Cohen, M.J., I.F. Creed, L. Alexander, N.B. Basu, A.J. Calhoun, C. Craft, E. D'Amico, E. DeKeyser, L. Fowler, and H.E. Golden. 2016. "Do Geographically Isolated Wetlands Influence Landscape Functions?" *Proceedings of the National Academy of Sciences of the United States of America* 113 (8): 1978–86.

Coles, A.E. 2017. "Runoff Generation Over Seasonally-Frozen Ground: Trends, Patterns, and Processes." PhD diss., University of Saskatchewan.

Creed, I.F., D.A. Aldred, J.N. Serran, and F. Accatino. 2017. "Maintaining the Portfolio of Wetland Functions on Landscapes: A Rapid Evaluation Tool for Estimating Wetland Functions and Values." In *Wetland and Stream Rapid Assessments: Development, Validation, and Application*, edited by J. Dorney, R. Savage, R.W. Tiner, and P. Adamus, 189–206. Amsterdam: Elsevier Publishing.

Dixon, M., J. Loh, N. Davidson, C. Beltrame, R. Freeman, and M. Walpole. 2016. "Tracking Global Change in Ecosystem Area: The Wetland Extent Trends Index." *Biological Conservation* 193: 27–35.

Evenson, G.R., H.E. Golden, C.R. Lane, D.L. McLaughlin, and E. D'Amico. 2018. "Depressional Wetlands Affect Watershed

Hydrological, Biogeochemical, and Ecological Functions." *Ecological Applications* 28 (4): 953–66.

Gleason, R.A., B.A. Tangen, M.K. Laubhan, K.E. Kermes, and N.H. Euliss, Jr. 2007. "Estimating Water Storage Capacity of Existing and Potentially Restorable Wetland Depressions in a Subbasin of the Red River of the North." USGS Northern Prairie Wildlife Research Center. http://digitalcommons.unl.edu/usgsnpwrc/89.

Golden, H.E., C.R. Lane, D.M. Amatya, K.W. Bandilla, H.R. Kiperwas, C.D. Knightes, and H. Ssegane. 2014. "Hydrologic Connectivity Between Geographically Isolated Wetlands and Surface Water Systems: A Review of Select Modeling Methods." *Environmental Modelling & Software* 53: 190–206.

Golden, H.E., H.A. Sander, C.R. Lane, C. Zhao, K. Price, E. D'Amico, and J.R. Christensen. 2015. "Relative Effects of Geographically Isolated Wetlands on Streamflow: A Watershed-Scale Analysis." *Ecohydrology* 9: 21–38.

Government of Alberta, 2013. "*Alberta Wetland Policy*." Government of Canada, Edmonton, Alberta, Canada.

Graf, J., E. Guzman, J. Hudson, L. Morningstar, M. Verleih, and S. Zhu. 2016. *Land Use Change in the Elbow River Watershed (from 1978–2015)*. Calgary, Alberta, Canada: University of Calgary.

Hayashi, M., and C.R. Farrow. 2014. "Watershed-Scale Response of Groundwater Recharge to Inter-Annual and Inter-Decadal Variability in Precipitation (Alberta, Canada)." *Hydrogeology Journal* 22 (8): 1825.

Hayashi, M., G. van der Kamp, and D.O. Rosenberry. 2016. "Hydrology of Prairie Wetlands: Understanding the Integrated Surface-Water and Groundwater Processes." *Wetlands* 36: 237–54.

Hubbard, D.E., and R.L. Linder. 1986. "Spring Runoff Retention in Prairie Pothole Wetlands." *Journal of Soil and Water Conservation* 41 (2): 122–25.

Johnson, W.C., and K.A. Poiani. 2016. "Climate Change Effects on Prairie Pothole Wetlands: Findings from a Twenty-Five Year Numerical Modeling Project." *Wetlands* 36 (2): 273–85.

Johnston, C.A., N.E. Detenbeck, and G.J. Niemi. 1990. "The Cumulative Effect of Wetlands on Stream Water Quality and Quantity. A Landscape Approach." *Biogeochemistry* 10 (2): 105–41.

Kusler, J.A., and M.E. Kentula. 1989. *Wetland Creation and Restoration: The Status of the Science*. Washington, DC: United States Environmental Protection Agency, Research and Development, Environmental Research Laboratory.

Lane, C.R., and E. D'Amico. 2010. "Calculating the Ecosystem Service of Water Storage in Isolated Wetlands Using LiDAR in North Central Florida, USA." *Wetlands* 30 (5): 967–77.

Lindsay, J.B., and I.F. Creed. 2005. "Sensitivity of Digital Landscapes to Artifact Depressions in Remotely-Sensed DEMs." *Photogrammetric Engineering & Remote Sensing* 71 (9): 1029–36.

Manning, R., J.P. Griffith, T. Pigot, and L.F. Vernon-Harcourt. 1890. *On the Flow of Water in Open Channels and Pipes*. Dublin, Ireland: Institution of Civil Engineers of Ireland.

Millett, B., W.C. Johnson, and G. Guntenspergen. 2009. "Climate Trends of the North American Prairie Pothole Region 1906–2000." *Climatic Change* 93 (1–2): 243–67.

Min, J.-H., D.B. Perkins, and J.W. Jawitz. 2010. "Wetland-Groundwater Interactions in Subtropical Depressional Wetlands." *Wetlands* 30 (5): 997–1006.

Moraghan, J. 1993. "Loss and Assimilation of 15N-Nitrate Added to a North Dakota Cattail Marsh." *Aquatic Botany* 46 (3–4): 225–34.

Morley, T.R., A.S. Reeve, and A.J. Calhoun. 2011. "The Role of Headwater Wetlands in Altering Streamflow and Chemistry in a Maine, USA Catchment." *Journal of the American Water Resources Association* 47 (2): 337–49.

Niazi, A., L.R. Bentley, and M. Hayashi. 2017. "Estimation of Spatial Distribution of Groundwater Recharge from Stream Baseflow and Groundwater Chloride." *Journal of Hydrology* 546: 380–92.

Phillips, J.V., and S. Tadayon. 2006. *Selection of Manning's Roughness Coefficient for Natural and Constructed Vegetated and Non-Vegetated Channels, and Vegetation Maintenance Plan Guidelines for Vegetated Channels in Central Arizona*. Washington, DC: US Department of the Interior, US Geological Survey.

Pomeroy, J.W., R.E. Stewart, and P.H. Whitfield. 2016. "The 2013 Flood Event in the South Saskatchewan and Elk River Basins: Causes, Assessment and Damages." *Canadian Water Resources Journal* 41 (1–2): 105–17.

Price, J.S., B.A. Branfireun, J. Michael Waddington, and K.J. Devito. 2005. "Advances in Canadian Wetland Hydrology, 1999–2003." *Hydrological Processes* 19 (1): 201–14.

Rains, M., S. Leibowitz, M. Cohen, I. Creed, H. Golden, J. Jawitz, P. Kalla, C. Lane, M. Lang, and D. McLaughlin. 2015. "Geographically Isolated Wetlands Are Part of the Hydrological Landscape." *Hydrological Processes* 30 (1): 153–60.

Rains, M.C. 2011. "Water Sources and Hydrodynamics of Closed-Basin Depressions, Cook Inlet Region, Alaska." *Wetlands* 31 (2): 377–87.

Serran, J.N., and I.F. Creed. 2016. "New Mapping Techniques to Estimate the Preferential Loss of Small Wetlands on Prairie Landscapes." *Hydrological Processes* 30: 396–409.

Serran, J.N., I.F. Creed, A.A. Ameli, and D.A. Aldred, 2018. Estimating Rates of Wetland Loss Using Power-Law Functions. *Wetlands* 38(1):109–20.

Therrien, R., R. McLaren, E. Sudicky, and S. Panday. 2008. *HydroGeoSphere: A Three-Dimensional Numerical Model Describing Fully-Integrated Subsurface and Surface Flow and Solute Transport*. Waterloo, ON: Groundwater Simulations Group.

USEPA. 2015. *Connectivity of Streams and Wetlands to Downstream Waters: A Review and Synthesis of the Scientific Evidence*. Washington, D.C.: US Environmental Protection Agency.

van der Kamp, G., and M. Hayashi. 2009. "Groundwater-Wetland Ecosystem Interaction in the Semiarid Glaciated Plains of North America." *Hydrogeology Journal* 17 (1): 203–14.

Waz, A., and I.F. Creed. 2017. "Automated Techniques to Identify Lost and Restorable Wetlands in the Prairie Pothole Region." *Wetlands* 37 (6): 1079–91.